G_1 and G_2 cell-cycle arrest following microtubule depolymerization in human breast cancer cells

April L. Blajeski,[1] Vy A. Phan,[2] Timothy J. Kottke,[3] and Scott H. Kaufmann[1,2,3]

[1]Department of Molecular Pharmacology and Experimental Therapeutics,
[2]Tumor Biology Program, Mayo Graduate School, and
[3]Division of Oncology Research, Mayo Clinic, Rochester, Minnesota, USA

Microtubule-depolymerizing agents are widely used to synchronize cells, screen for mitotic checkpoint defects, and treat cancer. The present study evaluated the effects of these agents on normal and malignant human breast cell lines. After treatment with 1 μM nocodazole, seven of ten breast cancer lines (type A cells) arrested in mitosis, whereas the other three (type B cells) did not. Similar effects were observed with 100 nM vincristine or colchicine. Among five normal mammary epithelial isolates, four exhibited type A behavior and one exhibited type B behavior. Further experiments revealed that the type B cells exhibited a biphasic dose-response curve, with mitotic arrest at low drug concentrations (100 nM nocodazole or 6 nM vincristine) that failed to depolymerize microtubules and a p53-independent $p21^{waf1/cip1}$-associated G_1 and G_2 arrest at higher concentrations (1 μM nocodazole or 100 nM vincristine) that depolymerized microtubules. Collectively, these observations provide evidence for coupling of premitotic cell-cycle progression to microtubule integrity in some breast cancer cell lines (representing a possible "microtubule integrity checkpoint") and suggest a potential explanation for the recently reported failure of some cancer cell lines to undergo nocodazole-induced mitotic arrest despite intact mitotic checkpoint proteins.

J. Clin. Invest. **110**:91–99 (2002). doi:10.1172/JCI200213275.

Introduction

Nocodazole, vincristine, and colchicine are structurally diverse agents that disrupt microtubule function by binding to various sites on β-tubulin and suppressing microtubule dynamics or inducing microtubule depolymerization (1–3). These actions are useful in cell synchronization studies, where brief exposures to nocodazole are routinely used to reversibly arrest cells in mitosis (4, 5). In addition, vinca alkaloids are used to treat several neoplasms (3), including breast cancer.

Microtubule-disrupting agents are thought to arrest cells in mitosis by triggering the mitotic checkpoint, a series of biochemical reactions that ensure proper attachment of chromosomes to the mitotic spindle before cells enter anaphase (reviewed in refs. 6–9). When microtubules fail to attach to one or more kinetochores as a result of drug treatment, components of the checkpoint continue to generate signals that inhibit the metaphase/anaphase transition.

Received for publication May 15, 2001, and accepted in revised form May 23, 2002.

Address correspondence to: Scott H. Kaufmann, Guggenheim 1301, Mayo Clinic, 200 First Street SW, Rochester, Minnesota 55905, USA. Phone: (507) 284-8950; Fax: (507) 284-3906; E-mail: kaufmann.scott@mayo.edu.

Conflict of interest: No conflict of interest has been declared.

Nonstandard abbreviations used: cyclin-dependent kinase (Cdk); Cdk inhibitor $p21^{Waf1/Cip1}$ (p21); human mammary epithelial cells (HMECs); propidium iodide (PI); bromodeoxyuridine (BrdU).

Like most cell-cycle checkpoints, the mitotic checkpoint can adapt. After prolonged treatment with microtubule-disrupting agents, cells exit mitosis without undergoing cytokinesis. These cells then enter an abnormal, tetraploid G_1-like phase (10–13) in which they are susceptible to activation of a "microtubule-sensitive" G_1 checkpoint (11, 14, 15) that results in p53-mediated upregulation of the cyclin-dependent kinase (Cdk) inhibitor $p21^{Waf1/Cip1}$ (p21) (16–20). p21 in turn inhibits the activity of Cdk2- and Cdk4-cyclin complexes, thereby arresting the cells in a tetraploid G_1 state (reviewed in ref. 21).

In addition to arresting cells in G_1, p21 can inhibit Cdc2–cyclin B complexes (21) and proliferating cell nuclear antigen (22–24), preventing interaction of the latter with other components of the DNA polymerase complex. One or both of these actions can contribute to a G_2 arrest following ectopic p21 expression or DNA damage (25, 26). Previous studies have not, however, implicated p21 in premitotic G_1 or G_2 arrests after microtubule disruption.

In the present work, we examined the effects of microtubule-depolymerizing agents on a series of human breast cancer cell lines and normal human mammary epithelial cells (HMECs), using conditions previously reported to identify cancer cell lines harboring mitotic checkpoint defects (27–30). Our results indicate that HMEC and breast cancer cell lines can be divided into two groups, those that respond with the expected mitotic arrest and those that do not. To our surprise, these differences reflected a previously undescribed p21-associated premitotic G_1 and G_2 arrest that

prevented some of the cell lines from ever reaching mitosis. These observations suggest that the effects of a whole class of widely used pharmacological agents are more complicated than previously suspected.

Methods

Materials. Nocodazole, vincristine, and colchicine were purchased from Sigma-Aldrich (St. Louis, Missouri, USA). Taq polymerase and reverse transcriptase were obtained from Roche Molecular Biochemicals (Indianapolis, Indiana, USA) and Promega Corp. (Madison, Wisconsin, USA), respectively. Murine monoclonal antibodies were purchased as follows: anti-cyclin B from Oncogene Research Products (Cambridge, Massachusetts, USA), anti-GADD45 from Santa Cruz Biotechnology Inc. (Santa Cruz, California, USA), anti–α-tubulin from Amersham Pharmacia Biotech (Piscataway, New Jersey, USA), and anti-p53 (clone 1801) and anti-p21 (Ab-11) from NeoMarkers (Fremont, California, USA). T. Yen (Fox Chase Cancer Center, Philadelphia, Pennsylvania, USA) and R. Abraham (Burnham Institute, La Jolla, California, USA) provided antisera to CENP-F and cyclin E, respectively. All other reagents were obtained as recently described (31).

Cell culture and determination of mitotic index. Breast cancer lines from American Type Culture Collection (Manassas, Virginia, USA) and low-passage HMECs from Clonetics Corp. (Walkersville, Maryland, USA) were cultured in the media designated by the suppliers. After treatment with drugs (prepared as 1,000-fold concentrated stocks in dimethyl sulfoxide) as described in the figure legends, adherent and nonadherent cells were combined, sedimented at 200 *g*, and incubated in 75 mM KCl for 15 minutes at 37°C. Cells were then fixed in 3.7% formaldehyde, washed with calcium- and magnesium-free PBS (32), sedimented onto glass slides at 90 *g*, stained with 1 μg/ml Hoechst 33258, and examined by fluorescence microscopy. At least 300 nuclei per sample were scored as interphase, mitotic, or apoptotic.

Cell-cycle analysis. After sedimentation at 200 *g* for 10 minutes, cells were washed with ice-cold PBS, fixed in 50% (vol/vol) ethanol, treated with 1 mg/ml RNase A, stained with 100 μg/ml propidium iodide (PI), and subjected to flow cytometry (33). DNA histograms were analyzed using ModFit software (Verity Software House Inc., Topsham, Maine, USA). For cell sorting experiments, cells containing 2N or 4N DNA were separated based on PI fluorescence using a FACSVantage SE (Becton, Dickinson and Co., San Jose, California, USA) and prepared for SDS-PAGE as described below. For bromodeoxyuridine (BrdU) incorporation studies, cells were pulsed with 20 μM BrdU for 20 minutes, washed, and treated with 1 μM nocodazole or 100 nM vincristine for 18 or 24 hours. After treatment, cells were trypsinized, centrifuged at 200 *g*, washed in ice-cold PBS, fixed in 66% (vol/vol) ethanol at –20°C, labeled with anti-BrdU antibody followed by PI, and subjected to flow cytometry as recently described (31).

Immunoblotting. Cells were washed twice with PBS and lysed in 6 M guanidine hydrochloride containing 250 mM Tris-HCl (pH 8.5 at 21°C), 10 mM EDTA, 150 mM β-mercaptoethanol, and 1 mM PMSF. After sonication and alkylation, samples were dialyzed into SDS and lyophilized (33). Aliquots containing 50 μg of total cellular protein were subjected to SDS-PAGE on 12% (wt/vol) polyacrylamide gels, transferred to nitrocellulose, and probed with antibodies as described (33).

Indirect immunofluorescence. Cells growing on coverslips were treated with nocodazole or vincristine for 8–24 hours as indicated in the figure legends. For CENP-F staining, coverslips were fixed in cold methanol for 20 minutes, air dried, and immediately washed once in PBS. For tubulin or cyclin B staining, samples were fixed in 3.7% formaldehyde and permeabilized in 0.1% Triton X-100. For all stains, coverslips were incubated overnight at 4°C in blocking buffer consisting of 10% (wt/vol) powdered milk, 150 mM NaCl, 10 mM Tris-HCl (pH 7.4 at 21°C), 100 U/ml penicillin, 100 μg/ml streptomycin, and 1 mM sodium azide; treated with primary antibodies for 1 hour in a humidified chamber at 37°C; washed three times in PBS; incubated with FITC-conjugated secondary antibodies for 1 hour at 37°C; washed in PBS; and counterstained with 0.5 μg/ml Hoechst 33258. Samples were photographed using MetaMorph computer software (Universal Imaging Corp., West Chester, Pennsylvania, USA) and a Hamamatsu C4742 digital camera (Hamamatsu Corp., Bridgewater, New Jersey, USA) mounted on a Zeiss IM35 microscope (Carl Zeiss Inc., Thornwood, New York, USA).

RT-PCR. After 2-μg aliquots of poly(A)$^+$ RNA were reverse transcribed, 1/25 of the resulting cDNA was used for each amplification. Following initiation under hot start conditions, PCR reactions were continued for 28 cycles on a PE 480 thermal cycler (PE Biosystems, Foster City, California, USA) using 92°C for denaturation, 55°C for annealing, and 72°C for extension (1 min/step). The following primers were used: p21 forward, 5′-CCTGCCGAAGTCAGTTCC-3′ and p21 reverse, 5′-CTGTGGGCGGATTAGGGC-3′; β-actin forward, 5′-GTGGGGCGCCCCAGGCACCA-3′ and β-actin reverse, 5′-CTCCTTAATGTCACGCACGATTTC-3′. Amplified products were separated on a 1% agarose gel, visualized under UV light, and sequenced to confirm their identity.

Results

Two types of cellular responses following treatment with 1 μM nocodazole or 100 nM vincristine. In experiments designed to search for mitotic checkpoint dysfunction, the ability of 1 μM nocodazole to produce mitotic arrest was examined in ten breast cancer cell lines. Seven of these cell lines (MCF-7, MDA-MB-231, MDA-MB-436, MDA-MB-453, HS0578T, SKBr3, and ZR-75-10) exhibited the expected mitotic arrest, with an increase in mitotic index of tenfold or more, and mean mitotic indices in excess of 20% after nocodazole exposure in each line. The mitotic index of MCF-7 cells, for example, increased from 2.2% ± 1.4% in diluent to 39% ± 11% (mean ± SD of 11 separate experiments) after 16–24

hours in nocodazole (Figure 1, a and b). In contrast, three cell lines (MDA-MB-468, BT20, and T47D) displayed a much less prominent mitotic arrest, with two- to fourfold increases in mitotic index, and mean mitotic indices below 10% after nocodazole treatment. The mitotic index of MDA-MB-468 cells, for example, increased from 2.4% ± 1.4% to 8.1% ± 3.5% (n = 13) after 16–24 hours in nocodazole. Results obtained with two lines that displayed prominent mitotic arrest (which we will designate "type A" cells) and two that did not ("type B" cells) are shown in Figure 1b. A similar dichotomy was observed when these four cell lines were treated with 100 nM vincristine (Figure 1c) or 100 nM colchicine (data not shown).

Cell-cycle effects of paclitaxel. One potential explanation for failure of some lines to arrest in mitosis would be the presence of mitotic checkpoint dysfunction. If this were the case, these cell lines should also fail to arrest in mitosis when treated with paclitaxel, an agent that activates the mitotic checkpoint (34, 35) by suppressing microtubule dynamics at low concentrations and causing tubulin hyperpolymerization at high concentrations (36). Contrary to this prediction, all the cell lines displayed a robust mitotic arrest during paclitaxel treatment (Figure 1d and data not shown).

In further experiments, basal levels of the mitotic checkpoint proteins BUB1, BUBR1, BUB3, MAD2, and p55Cdc20 were examined in all ten cell lines. Aside from the previously reported (28) low levels of MAD2 in T47D cells, there were no obvious defects in these mitotic checkpoint components that could explain the behavior of the type B cells (data not shown).

Another potential explanation for the failure to arrest in mitosis would be the occurrence of inefficient drug uptake or excessive drug efflux. As will be illustrated below (see Figure 6c), α-tubulin staining demonstrated microtubule depolymerization in type B cells treated with nocodazole, vincristine, or colchicine (data not shown), suggesting that the drugs were present and active within these cells.

Response of HMECs to microtubule-directed agents. Additional experiments examined the mitotic indices of normal HMECs after treatment with nocodazole, vincristine, or paclitaxel. For the HMEC isolate depicted in Figure 1e, each agent arrested a similar number of cells in mitosis. Similar results were observed with three additional independent HMEC isolates. In contrast, one isolate showed type B behavior that is characterized in greater detail below (see Figure 5c and accompanying text).

Nocodazole induces G_1 and G_2 arrest in MDA-MB-468 cells. Further experiments were performed to investigate the mechanistic basis for behavior of type B cells. Consistent with the mitotic arrest seen in Figure 1d, flow cytometry indicated that paclitaxel caused the MDA-MB-468 cells to accumulate in a tetraploid (4N) state (Figure 2b). In contrast, 1 μM nocodazole or 100 nM vincristine caused accumulation of cells in both 2N and 4N states, while the percentage of cells in S phase decreased (Figure 2, c and d). In additional experiments, similar results were observed in BT20 and T47D cells. These results raised the possibility that nocodazole or vincristine might cause these cells to arrest in both G_1 and G_2 before they ever reach mitosis.

To confirm that the 2N cells present after nocodazole and vincristine treatment resulted from G_1 arrest rather than progression of 4N cells through mitosis and cytokinesis, we pulsed MDA-MB-468 cells with 20 μM BrdU and determined whether the labeled S phase cells arrested in G_2 or continued through mitosis to the next G_1 phase. When diluent was added after BrdU labeling, about 68% of the labeled cells were found to be in G_1 18

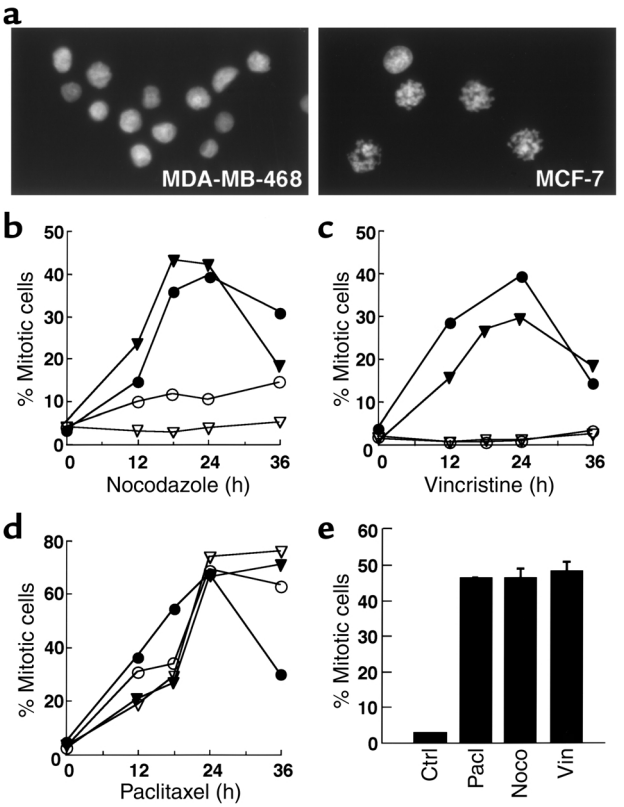

Figure 1
Two types of behavior following treatment of human breast cancer cell lines with microtubule-depolymerizing agents. (**a**) After a 24-hour treatment with 1 μM nocodazole, adherent and nonadherent MDA-MB-468 or MCF-7 cells were combined, stained with Hoechst 33258, and examined by fluorescence microscopy. Note that MDA-MB-468 cells remained in interphase, whereas many MCF-7 cells arrested in mitosis. (**b**–**d**) Breast cancer cells (filled triangles, MCF-7; filled circles, HS0578T; open triangles, BT20; open circles, MDA-MB-468) were treated with 1 μM nocodazole (**b**), 100 nM vincristine (**c**), or 100 nM paclitaxel (**d**) for various periods of time. Alternatively, HMECs (**e**) were treated with these agents for 14 hours, a length of time chosen because this isolate doubled every 16 hours. After adherent and nonadherent cells were combined, the morphology of 300 or more nuclei in each sample was scored by fluorescence microscopy. In **b**–**d**, representative individual experiments are shown and the degree of variation is indicated in the text. In **e**, the mean and range of two experiments are shown. Ctrl, control; Pacl, paclitaxel; Noco, nocodazole; Vin, vincristine.

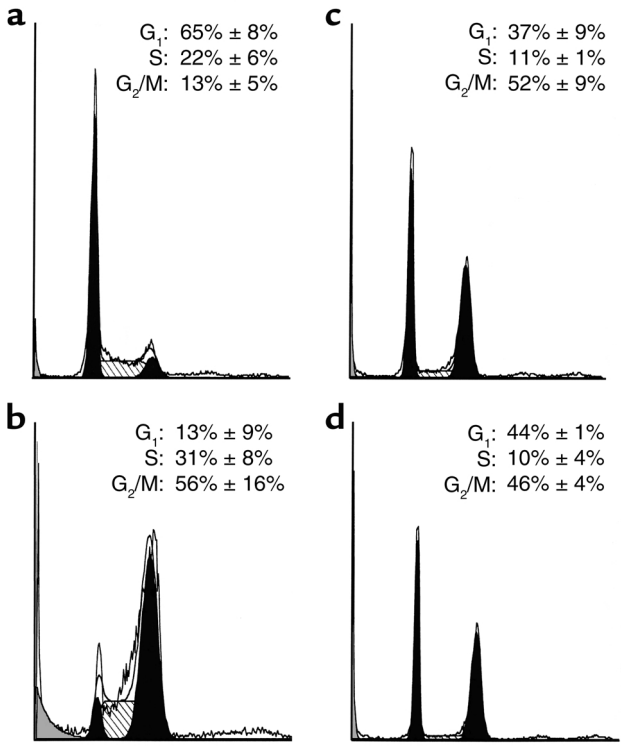

Figure 2
MDA-MB-468 cells arrest in G_1 and G_2 following nocodazole and vincristine treatment. Cells treated with diluent (**a**), 100 nM paclitaxel (**b**), 1 μM nocodazole (**c**), or 100 nM vincristine (**d**) for 24 hours were stained with PI and subjected to flow cytometry. Numbers in each panel show mean ± SD of distributions inferred from PI staining of three to six separate experiments using ModFit.

hours later (Table 1, control). In contrast, only 5% of the labeled cells progressed through mitosis to G_1 when nocodazole or vincristine was added for 18 or 24 hours after BrdU labeling (Table 1). These results indicated that cells in S phase at the time of labeling arrested in a 4N state and failed to contribute to the 2N population, suggesting that the 2N population detected after drug treatment must have originated from cells that were already in G_1.

To determine whether the 4N cells were arrested in G_2 or the tetraploid G_1-like state observed when cells exit mitosis in the presence of microtubule-disrupting agents (10–13), cells were stained with reagents that recognize polypeptides present during G_2 but not G_1. The kinetochore protein CENP-F displays focal nuclear localization only during late G_2 (37, 38). The percentage of MDA-MB-468 cells containing focal CENP-F staining increased dramatically after treatment with nocodazole or vincristine (Figure 3, b, c, and g). This staining was similar in distribution but more intense than that observed in untreated cells (Figure 3a) or following γ-irradiation, which activates a G_2 DNA damage checkpoint (data not shown). Cyclin B, which accumulates in late S and G_2 phases, remains localized to the cytoplasm until cells undergo G_2/M transition (39, 40). After treatment with nocodazole or vincristine, cyclin B was detected in a cytoplasmic pattern (Figure 3, e and f) similar to that observed following γ-irradiation (data not shown). These results suggest that 4N cells were arrested in late G_2. Combined with the results in Figure 2 and Table 1, these observations indicate that type B cells arrested in both G_1 and G_2 following treatment with 1 μM nocodazole and therefore never reached mitosis.

Upregulation of p21 in type B cells during nocodazole-induced G_1 and G_2 arrest. A common mechanism of cell-cycle arrest involves upregulation of endogenous Cdk inhibitors, including $p27^{Kip1}$ and p21, which prevent cell-cycle progression by blocking Cdk activity (reviewed in ref. 21). Immunoblotting indicated that $p27^{Kip1}$ levels in MDA-MB-468 cells did not change after nocodazole treatment (data not shown). In contrast, p21 levels increased dramatically following a 24-hour exposure to nocodazole, vincristine, or colchicine (Figure 4a). Importantly, p21 did not increase during paclitaxel treatment (Figure 4a), which induced a mitotic arrest (Figure 1d). Further examination revealed that p21 mRNA (Figure 4b) and protein (Figure 4c) increased within 4 hours of addition of nocodazole. Because MDA-MB-468 cells contain mutated, functionally inactive p53 (41), the observed p21 upregulation appeared to be p53-independent. Consistent with this conclusion, the p53-regulated protein GADD45 did not increase after nocodazole (Figure 4c).

To determine which cells contained elevated levels of p21 protein after nocodazole treatment, MDA-MB-468 cells were separated into 2N and 4N populations based on PI staining (Figure 4d). Immunoblotting (Figure 4e) revealed that cyclin E levels were high in the 2N population and cyclin B levels were high in the 4N population, confirming the accuracy of the sorting process. In contrast, p21 was elevated in both populations, suggesting its possible role in both the G_1 and G_2 arrests.

Dose-dependent effect of nocodazole on type B cells. Although the 1-μM nocodazole concentration used in the preceding experiments was within the range previously used to evaluate mitotic checkpoint function (27–30), the failure of three lines to arrest in mitosis appeared to be at odds with the widespread use of nocodazole as a synchronizing agent in cell biology studies. In an attempt to reconcile these observations, we examined the effects of varying nocodazole and vincristine concentrations. Interestingly, MDA-MB-468 (type B) cells arrested in mitosis at low drug con-

Table 1
Cell-cycle distribution of BrdU-pulsed cells after microtubule disruption

% cells with 2N DNA after:	18 h	24 h
Control	68.1 ± 12.0	75.5 ± 18.7
Nocodazole	4.9 ± 2.9	6.5 ± 0.8
Vincristine	5.2 ± 2.7	6.6 ± 4.3

MDA-MB-468 cells were pulsed with 20 μM BrdU for 20 minutes, washed, and incubated in the absence (control) or presence of 1 μM nocodazole or 100 nM vincristine for various periods of time. The cell-cycle distribution of labeled, adherent cells was examined as described in Methods. Results are mean ± SD of three independent experiments.

centrations, e.g., 150–300 nM nocodazole (Figure 5a) or 6–12 nM vincristine (data not shown), even though these cells did not arrest at higher concentrations (Figure 1, a–c). Similar results were observed with T47D cells (Figure 5b), BT20 cells (not shown), and an HMEC isolate that exhibited type B behavior (Figure 5c). This mitotic arrest at low concentrations suggests that intrinsic mitotic checkpoint defects or altered drug accumulation are unlikely to account for the behavior of type B cells at higher drug concentrations. In contrast, numerous type A cells, including MCF-7, MDA-MB-231, MDA-MB-453, ZR-75-10, and SKBr3 cells, exhibited a robust mitotic arrest when treated with nocodazole concentrations ranging up to 30 μM (Figure 5d and data not shown). These observations rule out the possibility that type B behavior can be elicited in type A cells by merely increasing the drug concentration. Instead, it appears that breast cancer cells will arrest in mitosis following exposure to low or high doses of nocodazole unless other events (e.g., G_1 and G_2 arrest) intervene and prevent the cells from reaching M phase.

To determine whether similar dose-dependent effects might be observed with paclitaxel, mitotic indices were determined after MDA-MB-468 cells were treated for 22–24 hours with paclitaxel at concentrations ranging from 100 nM to 10 μM. Results of this analysis (Figure 5e) failed to provide evidence for diminished mitotic arrest at high drug concentrations. Instead, the premitotic arrest observed in type B cells appeared to be limited to microtubule-destabilizing agents.

To further evaluate the potential role of p21 in the nocodazole-induced G_1 and G_2 arrests, p21 levels were examined in MDA-MB-468 cells treated with varying concentrations of nocodazole. p21 consistently increased in MDA-MB-468 cells only at nocodazole concentrations (300–1,000 nM) that inhibited mitotic arrest (Figure 5f). When multiple cell lines were examined after treatment with 1 μM nocodazole, p21 was also elevated in BT20 and T47D cells (Figure 5g), which exhibited type B behavior, but not in MCF-7, MDA-MB-231, MDA-MB-453, or SKBr3 cells (Figure 5h and data not shown), which exhibited type A behavior.

Relationship between cell-cycle arrest and microtubule depolymerization. Because low doses of nocodazole and vincristine reportedly stabilize microtubule dynamics without any significant decrease in microtubule polymer mass (42, 43), whereas higher concentrations induce microtubule depolymerization in HeLa cells (10, 43), we assessed the possibility that these two processes correspond to the two types of behavior by studying α-tubulin localization after treatment with low or high concentrations of nocodazole. Results obtained in MDA-MB-468 and MCF-7 cells are shown for purposes of illustration (Figure 6). After treatment with 167 nM nocodazole, which induced mitotic arrest (Figure 1b and Figure 5a), numerous microtubules were present in both cell lines (Figure 6, b and e). This is consistent with the stabilization of microtubule dynamics without any alteration in microtubule mass (43). After treatment with 1 μM nocodazole, however, microtubules in the two cell lines exhibited different behaviors: intact microtubules could still be observed in MCF-7 cells (Figure 6f) but not in MDA-MB-468 cells (Figure 6c). Experiments in other cell lines, however, ruled out the possibility that these different microtubule behaviors correlate with cell-cycle response. Although other type B cells (T47D, BT20, and the HMEC isolate shown in Figure 5c) also displayed extensive microtubule depolymerization at 1-3

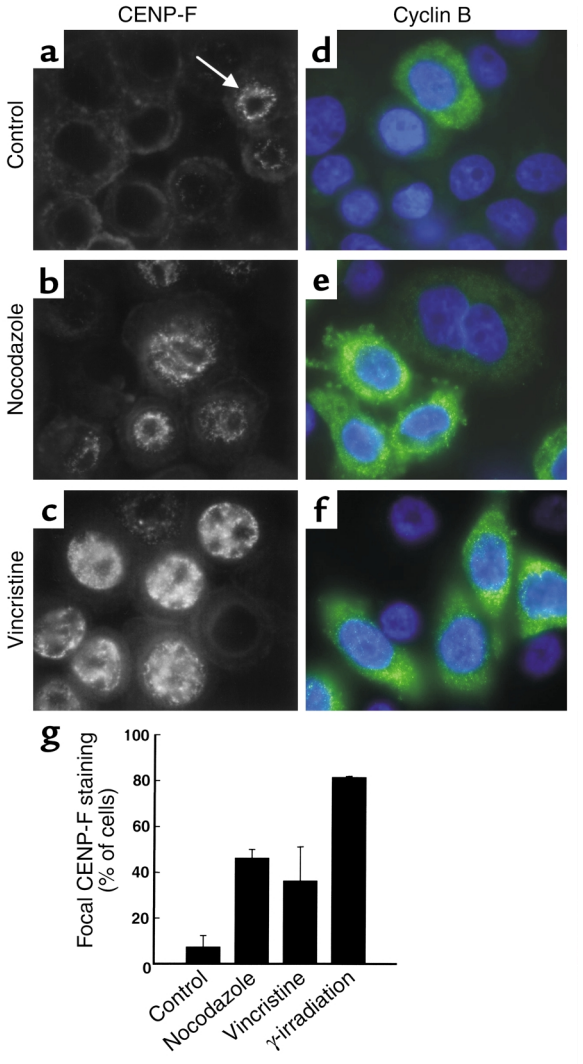

Figure 3
A subset of MDA-MB-468 cells arrest in late G_2 following nocodazole or vincristine treatment. Cells growing on coverslips were treated with diluent (**a** and **d**), 1 μM nocodazole (**b** and **e**), or 100 nM vincristine (**c** and **f**) for 24 hours, then fixed and stained with antibodies to CENP-F (**a**–**c**) or cyclin B (**d**–**f**). (**g**) The percentage of cells displaying focal nuclear CENP-F localization (arrow in **a**) increased after a 24-hour treatment with nocodazole or vincristine. Results shown are mean ± SD of three separate experiments. Ionizing radiation was used as a positive control. Quantitative analysis demonstrated that the number of cells with cytoplasmic cyclin B localization increased in a very similar fashion.

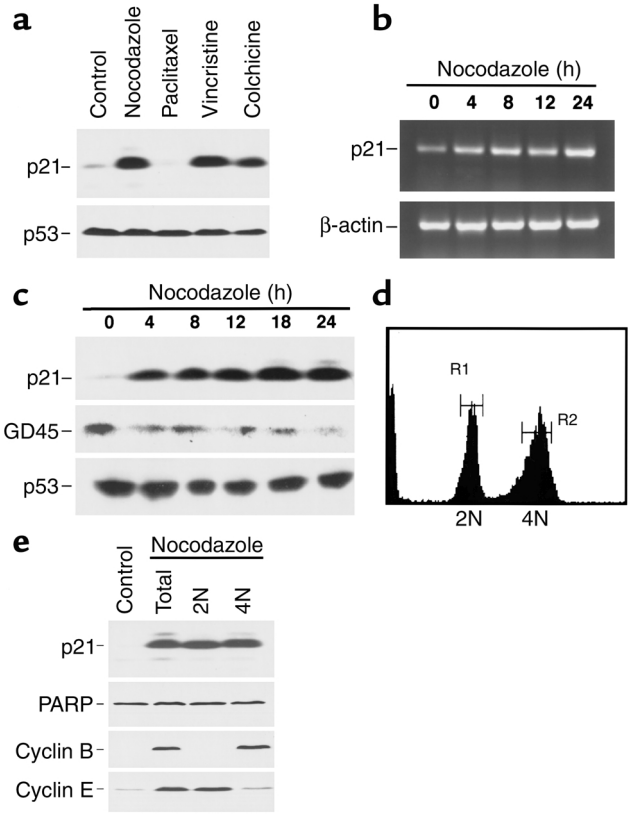

Figure 4
Increased p21 expression after treatment of MDA-MB-468 cells with microtubule-depolymerizing agents. (**a**) Cells were treated with 1 μM nocodazole, 100 nM paclitaxel, 100 nM vincristine, or 100 nM colchicine for 24 hours. Whole-cell lysates were subjected to SDS-PAGE and probed for p21. p53, which is mutated in these cells (41), served as a loading control. (**b**) Poly(A)$^+$ RNA from cells treated with 1 μM nocodazole for various periods of time was analyzed by RT-PCR using primers specific for p21. β-actin served as a control. (**c**) Cells were treated with 1 μM nocodazole for various lengths of time before SDS-PAGE and immunoblotting for p21, GADD45 (GD45), or p53 (as a loading control). (**d** and **e**) Cells were treated with 1 μM nocodazole for 24 hours, fixed in 50% ethanol, stained with PI, and sorted into 2N and 4N populations by flow cytometry (gates set as shown). Protein (50 μg) from unsorted (total) or sorted (2N or 4N) cell populations was subjected to SDS-PAGE followed by immunoblotting. Cyclin B and cyclin E served as markers of the G_2 and G_1 populations, respectively, while PARP served as a loading control.

μM nocodazole (similar to Figure 6c), so did MDA-MB-453, MDA-MB-431, and an HMEC isolate that displayed type A behavior. Thus, G_1 and G_2 arrests occurred in type B cells at drug concentrations that depolymerized microtubules; but microtubule depolymerization did not guarantee type B behavior.

Discussion

In the present study, morphological analysis indicated that ten breast cancer cell lines could be divided into two groups: those that display a prominent mitotic arrest after treatment with 1 μM nocodazole, 100 nM vincristine, or 100 nM colchicine (type A cells), and those that do not (type B cells). Nontransformed HMECs exhibited a similar dichotomy. Further experiments demonstrated that type B cells arrest in mitosis at low drug concentrations but undergo p21-associated G_1 and G_2 arrests at higher drug concentrations. These results have potentially important implications for current understanding of the actions of spindle poisons.

Because type A cells exhibited the expected response to microtubule-depolymerizing agents, much of the present analysis focused on type B cells. Several observations suggested that these cells have intact mitotic checkpoints. First, type B cells arrested in mitosis after treatment with paclitaxel (Figure 1d, Figure 5c, and data not shown), another agent that activates the mitotic checkpoint (35, 44). Second, type B cells arrested in mitosis at lower concentrations of nocodazole, vincristine, or colchicine (Figure 5, a and b, and data not shown), demonstrating that the machinery responsible for mitotic arrest was functionally intact. Third, BrdU labeling (Table 1) and cyclin analysis (Figure 3e and Figure 4e) indicated that these cells failed to reenter G_1, a cell-cycle phase they would be expected to enter if the mitotic checkpoint malfunctioned.

Defects in the checkpoint protein Chfr also fail to account for the behavior of type B cells. Upon treatment with 1.5 μM nocodazole, 1.5 μM colcemid, or 5 μM paclitaxel during G_2, tumor cell lines lacking Chfr rapidly accumulate in mitosis, whereas cells expressing Chfr exhibit a 6-hour delay before entering mitosis (45). The failure of type B cells to accumulate in mitosis when followed for as long as 72 hours after treatment with 1 μM nocodazole or 100 nM vincristine (Figure 1, b and c, and data not shown) clearly distinguished type B cells from Chfr-deficient cells as well.

Further investigation revealed that MDA-MB-468 cells, a prototypic type B cell line, arrested in both G_1 and G_2 after treatment with 1 μM nocodazole or 100 nM vincristine. The presence of a G_1 arrest was indicated by the persistence of cells with 2N DNA content and high cyclin E levels (Figure 2, c and d, and Figure 4, d and e) despite the failure of 4N cells to undergo cytokinesis (Table 1). The presence of a G_2 arrest was indicated by the accumulation of 4N cells (Figure 2, c and d) with interphase morphology (Figure 1a and Figure 3), high levels of cytoplasmic cyclin B (Figure 3, e and f, and Figure 4e), and focal staining for CENP-F (Figure 3, b, c, and g). Although microtubule-disrupting agents have been observed to induce accumulation in a tetraploid G_1-like state following mitotic delay and abnormal mitotic exit (11, 14–20), to our knowledge this is the first report of premitotic G_1 and G_2 arrest induced by these agents.

These premitotic G_1 and G_2 arrests were associated with increased expression of p21 (Figure 4), a Cdk inhibitor that plays critical roles in G_1 and G_2 arrests after DNA damage (26, 46). Several observations raised the possibility that p21 might contribute to the behavior of the type B cells. First, elevated p21 levels were observed in both G_1 and G_2 cell populations (Figure

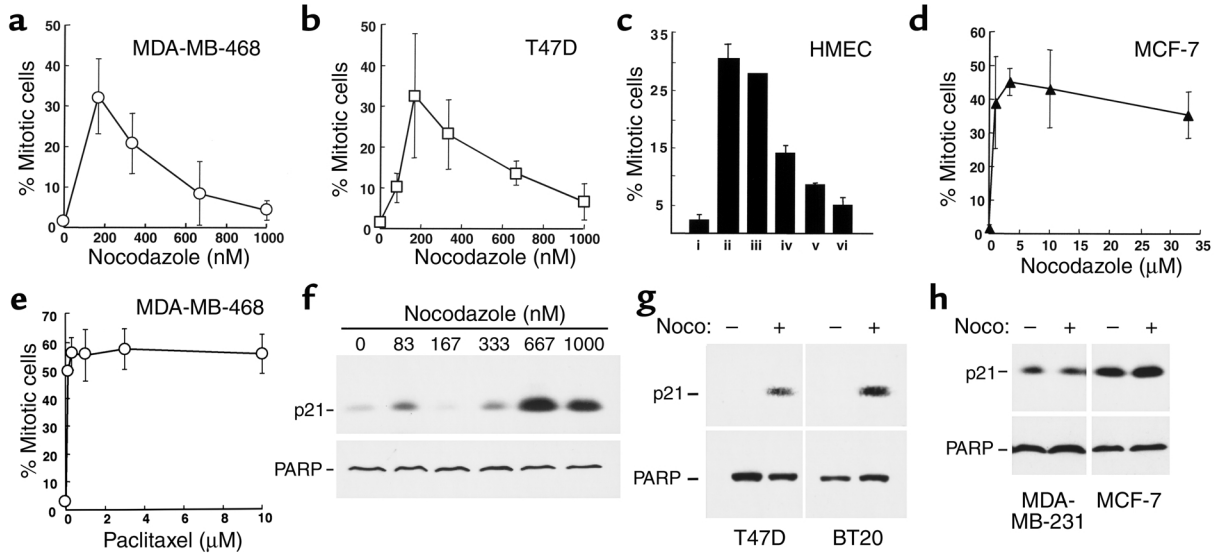

Figure 5
Dose-dependent mitotic arrest of type B cells during nocodazole treatment. (**a**–**d**) After a 24-hour treatment with various nocodazole concentrations, adherent and nonadherent MDA-MB-468 (**a**), T47D (**b**), or MCF-7 cells (**d**) were combined and examined by fluorescence microscopy. (**c**) HMECs (passages 2–4) were treated for 24 hours with diluent (i), 100 nM paclitaxel (ii), or nocodazole at 83, 167, 1,200, and 3,000 nM (iii–vi, respectively). (**e**) After a 24-hour treatment with various concentrations of paclitaxel, adherent and nonadherent MDA-MB-468 cells were combined and examined by fluorescence microscopy. (**f**–**h**) Whole-cell lysates from MDA-MB-468 cells treated with the indicated concentration of nocodazole for 24 hours (**f**), or the indicated cell lines treated with 1 μM nocodazole for 24 hours (**g** and **h**) were subjected to SDS-PAGE followed by blotting for p21 and PARP (which served as a loading control). Error bars show ± one SD from three independent experiments (**a**, **b**, **d**, and **e**), or ± range from two (**c**) independent experiments.

4e). Second, p21 levels increased after treatment with nocodazole, vincristine, or colchicine, but not paclitaxel, which failed to induce G_1 and G_2 arrests (Figure 1d and Figure 4a). Third, p21 levels were significantly elevated (four- to eightfold) only after treatment with nocodazole concentrations that caused the G_1 and G_2 arrests in type B cells (Figure 5, a and f). Finally, p21 levels increased in additional type B cells (Figure 5g) but not type A cells (Figure 5h). Although these observations establish a correlation between p21 elevation and the observed G_1 and G_2 arrests, more definitive evidence that p21 participates in type B behavior will require the examination of *p21*$^{-/-}$ cells. Unfortunately, parental cells corresponding to both currently available *p21*$^{-/-}$ cell lines (mouse fibroblasts and HCT116 colon cancer cells) exhibit type A behavior in response to nocodazole (refs. 27, 47, and data not shown), making these models unsuitable for assessing the role of p21 in the type B response.

The events leading from microtubule disturbance to p21 upregulation in type B cells require further study. The failure of other DNA damage–responsive polypeptides such as GADD45 to accumulate (Figure 4a) distinguishes nocodazole-induced p21 upregulation from a DNA damage response. Moreover, the accumulation of p21 in MDA-MB-468 cells, which contain mutant

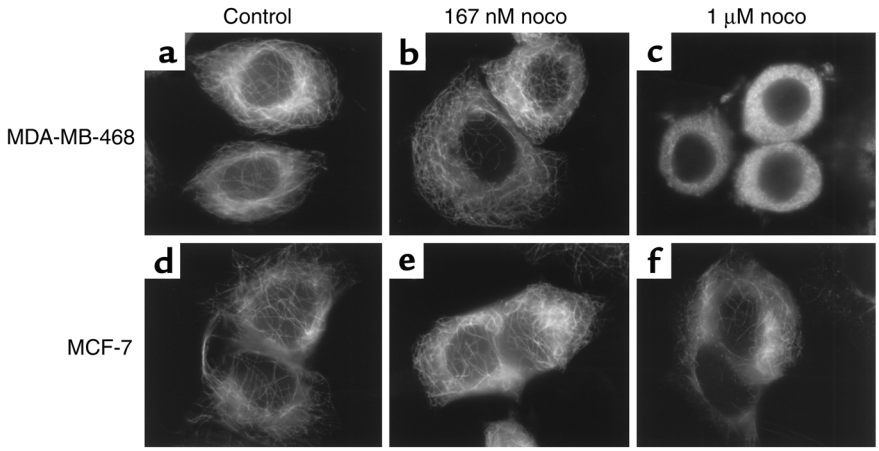

Figure 6
Effect of nocodazole on microtubule stability in MDA-MB-468 and MCF-7 cells. MDA-MB-468 (**a**–**c**) or MCF-7 (**d**–**f**) cells growing on coverslips were treated with diluent (**a** and **d**), 167 nM nocodazole (**b** and **e**), or 1 μM nocodazole (**c** and **f**) for 8 hours (by this time most MCF-7 cells had not yet accumulated in mitosis and thus remained adherent), fixed, stained with anti–α-tubulin, and visualized by fluorescence microscopy.

p53 (41), suggests that nocodazole-induced p21 upregulation does not depend on p53 function.

Consistent with this latter conclusion, no relationship between p53 status and nocodazole-induced cell-cycle effects was observed. In particular, cells with p53 mutations exhibited both type A (MDA-MB-231, SKBr3, HS0578T) and type B (MDA-MB-468, T47D) behavior. Likewise, as described above, differences in microtubule stability did not track with type A versus type B behavior. Instead, the observation that different HMEC isolates also exhibit this dichotomous behavior (Figure 1e and Figure 5c) raised the possibility that allelic polymorphism in a currently unidentified gene determines the cell-cycle response to microtubule disruption.

The results presented above have potentially important implications for current efforts to study mitotic checkpoint function in cancer cell lines. Recent studies have demonstrated that approximately 50% of colon cancer cell lines fail to arrest upon exposure to 0.7 μM nocodazole. Although *BUB1* mutations were demonstrated in two of these lines, extensive analysis failed to identify additional mutations in mitotic checkpoint genes in a variety of cancer cell lines (48–50). Our results indicate that the use of high-dose nocodazole to screen for mitotic checkpoint defects in breast cancer lines results in false positives because a number of lines arrest in G_1 and G_2 before reaching mitosis. Whether similar limitations apply to other cell types remains to be determined.

In summary, the present observations lead to a number of unexpected conclusions. First, microtubule-depolymerizing agents can cause simultaneous G_1 and G_2 arrests before some cells ever reach mitosis. Second, this type B phenotype correlates with p53-independent induction of p21. Third, type B behavior occurs in some HMEC isolates as well as breast cancer cell lines, raising the possibility that it reflects normal phenotypic variation rather than cancer-associated checkpoint loss. Collectively, these observations suggest that microtubule-depolymerizing agents have effects that are more complicated and more diverse than previously appreciated.

Acknowledgments

We thank Wilma Lingle for gifts of several HMEC isolates; Song Tao-Liu for collaborative work examining mitotic checkpoint proteins; Jeff Salisbury for use of his fluorescent microscope; Larry Karnitz, Tim Yen, Nita Maihle, Jann Sarkaria, Junjie Chen, and William C. Earnshaw for helpful discussions; and the anonymous reviewers for helpful suggestions. This work was supported in part by NIH grant R01 CA-69008 and predoctoral fellowships from the Mayo Foundation.

1. Jordan, M.A., and Wilson, L. 1998. Microtubules and actin filaments: dynamic targets for cancer chemotherapy. *Curr. Opin. Cell Biol.* **10**:123–130.
2. Downing, K.H. 2000. Structural basis for the interaction of tubulin with proteins and drugs that affect microtubule dynamics. *Ann. Rev. Cell Dev. Biol.* **16**:89–111.
3. Rowinsky, E.K., and Donehower, R.C. 2001. Antimicrotubule agents. In *Cancer chemotherapy and biotherapy.* B.A. Chabner and D.L. Longo, editors. Lippincott, Williams & Wilkins. Philadelphia, Pennsylvania, USA. 329–372.
4. Zieve, G.W., Turnbull, D., Mullins, J.M., and McIntosh, J.R. 1980. Production of large numbers of mitotic mammalian cells by use of the reversible microtubule inhibitor nocodazole. *Exp. Cell Res.* **126**:397–405.
5. De Brabander, M., Geuens, G., Nuydens, R., Willebrords, R., and De Mey, J. 1981. Microtubule assembly in living cells after release from nocodazole block: the effects of metabolic inhibitors, taxol and pH. *Cell Biol. Int. Rep.* **5**:913–920.
6. Rudner, A.D., and Murray, A.W. 1996. The spindle assembly checkpoint. *Curr. Opin. Cell Biol.* **8**:773–780.
7. Amon, A. 1999. The spindle checkpoint. *Curr. Opin. Genet. Dev.* **9**:69–75.
8. Burke, D.J. 2000. Complexity in the spindle checkpoint. *Curr. Opin. Genet. Dev.* **10**:26–31.
9. Shah, J.V., and Cleveland, D.W. 2000. Waiting for anaphase: Mad2 and the spindle assembly checkpoint. *Cell.* **103**:997–1000.
10. Jordan, M.A., Thrower, D., and Wilson, L. 1991. Mechanism of inhibition of cell proliferation by vinca alkaloids. *Cancer Res.* **51**:2212–2222.
11. Woods, C.M., Zhu, J., McQueney, P.A., Bollag, D., and Lazarides, E. 1995. Taxol-induced mitotic block triggers rapid onset of a p53-independent apoptotic pathway. *Mol. Med.* **1**:506–526.
12. Jordan, M.A., et al. 1996. Mitotic block induced in HeLa cells by low concentrations of paclitaxel (taxol) results in abnormal mitotic exit and apoptotic cell death. *Cancer Res.* **56**:816–825.
13. Torres, K., and Horwitz, S.B. 1998. Mechanisms of taxol-induced cell death are concentration dependent. *Cancer Res.* **58**:3620–3626.
14. Notterman, D., Young, S., Wainger, B., and Levine, A.J. 1998. Prevention of mammalian DNA reduplication following the release from the mitotic spindle checkpoint, requires p53 protein, but not p53-mediated transcriptional activity. *Oncogene.* **17**:2743–2751.
15. Casenghi, M., et al. 1999. p53-independent apoptosis and p53-dependent block of rereplication following mitotic spindle inhibition in human cells. *Exp. Cell Res.* **250**:339–350.
16. Barboule, N., Chadebech, P., Baldin, V., Vidal, S., and Valette, A. 1997. Involvement of p21 in mitotic exit after paclitaxel treatment in MCF-7 breast adenocarcinoma cell line. *Oncogene.* **15**:2867–2875.
17. Di Leonardo, et al. 1997. DNA rereplication in the presence of mitotic spindle inhibitors in human and mouse fibroblasts lacking either p53 or pRb function. *Cancer Res.* **57**:1013–1019.
18. Khan, S.H., and Wahl, G.M. 1998. p53 and pRb prevent rereplication in response to microtubule inhibitors by mediating a reversible G1 arrest. *Cancer Res.* **58**:396–401.
19. Lanni, J.S., and Jacks, T. 1998. Characterization of the p53-dependent postmitotic checkpoint following spindle disruption. *Mol. Cell. Biol.* **18**:1055–1064.
20. Stewart, Z.A., Mays, D., and Pietenpol, J.A. 1999. Defective G1-S cell cycle checkpoint function sensitizes cells to microtubule inhibitor-induced apoptosis. *Cancer Res.* **59**:3831–3837.
21. Vidal, A., and Koff, A. 2000. Cell-cycle inhibitors: three families united by a common cause. *Gene.* **247**:1–15.
22. Waga, S., Hannon, G.J., Beach, D., and Stillman, B. 1994. The p21 inhibitor of cyclin-dependent kinases controls DNA replication by interaction with PCNA. *Nature.* **369**:520–521.
23. Chen, J., Jackson, P.K., Kirschner, M.W., and Dutta, A. 1995. Separate domains of p21 involved in the inhibition of Cdk kinase and PCNA. *Nature.* **374**:386–388.
24. Luo, Y., Hurwitz, J., and Massague, J. 1995. Cell-cycle inhibition by independent CDK and PCNA binding domains of $p21^{Cip1}$. *Nature.* **375**:159–161.
25. Cayrol, C., Knibiehler, M., and Ducommun, B. 1998. p21 binding to PCNA causes G1 and G2 cell cycle arrest in p53-deficient cells. *Oncogene.* **16**:311–320.
26. Bunz, F., et al. 1998. Requirement for p53 and p21 to sustain G2 arrest after DNA damage. *Science.* **282**:1497–1501.
27. Cahill, D.P., et al. 1998. Mutations of mitotic checkpoint genes in human cancers. *Nature.* **392**:300–303.
28. Li, Y., and Benezra, R. 1996. Identification of a human mitotic checkpoint gene: hsMAD2. *Science.* **274**:246–248.
29. Dobles, M., Liberal, V., Scott, M.L., Benezra, R., and Sorger, P.K. 2000. Chromosome missegregation and apoptosis in mice lacking the mitotic checkpoint protein Mad2. *Cell.* **101**:635–645.
30. Michel, L.S., et al. 2001. MAD2 haplo-insufficiency causes premature anaphase and chromosome instability in mammalian cells. *Nature.* **409**:355–359.
31. Cliby, W.A., Lewis, K.A., Lilly, K.K., and Kaufmann, S.H. 2002. S phase and G_2 arrests induced by topoisomerase I poisons are dependent on ATR kinase function. *J. Biol. Chem.* **277**:1599–1606.

32. Blajeski, A.L., and Kaufmann, S.H. 2001. A multistep model for paclitaxel-induced apoptosis in human breast cancer cell lines. *Exp. Cell Res.* **270**:277–288.
33. Kottke, T.J., et al. 1999. Comparison of paclitaxel-5-fluoro-2′-deoxyuridine- and epidermal growth factor-induced apoptosis: evidence for EGF-induced anoikis. *J. Biol. Chem.* **274**:15927–15936.
34. Rieder, C.L., Cole, R.W., Khodjakov, A., and Sluder, G. 1995. The checkpoint delaying anaphase in response to chromosome monoorientation is mediated by an inhibitory signal produced by unattached kinetochores. *J. Cell Biol.* **130**:941–948.
35. Martinez-Exposito, M.J., Kaplan, K.B., Copeland, J., and Sorger, P.K. 1999. Retention of the BUB3 checkpoint protein on lagging chromosomes. *Proc. Natl. Acad. Sci. USA.* **96**:8493–8498.
36. Jordan, M.A., Toso, R.J., Thrower, D., and Wilson, L. 1993. Mechanism of mitotic block and inhibition of cell proliferation by taxol at low concentrations. *Proc. Natl. Acad. Sci. USA.* **90**:9552–9556.
37. Rattner, J.B., Rao, A., Fritzler, M.J., Valencia, D.W., and Yen, T.J. 1993. CENP-F is a .ca 400 kDa kinetochore protein that exhibits a cell-cycle dependent localization. *Cell Motil. Cytoskeleton.* **26**:214–226.
38. Liao, H., Winkfrein, R.J., Mack, G., Rattner, J.B., and Yen, T.J. 1995. CENP-F is a protein of the nuclear matrix that assembles onto kinetochores at late G2 and is rapidly degraded after mitosis. *J. Cell Biol.* **130**:507–518.
39. Pines, J., and Hunter, T. 1991. Human cyclins A and B1 are differentially located in the cell and undergo cell cycle-dependent nuclear transport. *J. Cell Biol.* **115**:1–17.
40. Hagting, A., Jackman, M., Simpson, K., and Pines, J. 1999. Translocation of cyclin B1 to the nucleus at prophase requires a phosphorylation-dependent nuclear import signal. *Curr. Biol.* **9**:680–689.
41. Nigro, J.M., et al. 1989. Mutations in the p53 gene occur in diverse human tumour types. *Nature.* **342**:705–708.
42. Jordan, M.A., Himes, R.H., and Wilson, L. 1985. Comparison of the effects of vinblastine, vincristine, vindesine, and vinepidine on microtubule dynamics and cell proliferation in vitro. *Cancer Res.* **45**:2741–2747.
43. Jordan, M.A., Thrower, D., and Wilson, L. 1992. Effects of vinblastine, podophyllotoxin and nocodazole on mitotic spindles. Implications for the role of microtubule dynamics in mitosis. *J. Cell Sci.* **102**:401–416.
44. Yvon, A.-M.C., Wadsworth, P., and Jordan, M.A. 1999. Taxol suppresses dynamics of individual microtubules in living human tumor cells. *Mol. Biol. Cell.* **10**:947–959.
45. Scolnick, D.M., and Halazonetis, T.D. 2000. Chrf defines a mitotic stress checkpoint that delays entry into metaphase. *Nature.* **406**:430–434.
46. El-Deiry, W.S., et al. 1993. WAF1, a potential mediator of p53 tumor suppression. *Cell.* **75**:817–825.
47. Elvin, P., and Evans, C.W. 1983. Cell adhesiveness and the cell cycle: correlation in synchronized Balb/c 3T3 cells. *Biol. Cell.* **48**:1–9.
48. Cahill, D.P., et al. 1999. Characterization of MAD2B and other mitotic spindle checkpoint genes. *Genomics.* **58**:181–187.
49. Yamaguchi, K., et al. 1999. Mutation analysis of hBUB1 in aneuploid HNSCC and lung cancer cell lines. *Cancer Lett.* **139**:183–187.
50. Myrie, K.A., Percy, M.J., Azim, J.N., Neeley, C.K., and Petty, E.M. 2000. Mutation and expression analysis of human BUB1 and BUB1B in aneuploid breast cancer cell lines. *Cancer Lett.* **152**:193–199.